JOURNAL OF CATALYSIS 83, 301–314 (1983)

Strong Metal–Support Interactions for Pt and Rh on Al_2O_3 and TiO_2: Application of Nuclear Backscattering Spectrometry

J. A. CAIRNS,[1] J. E. E. BAGLIN, G. J. CLARK, AND J. F. ZIEGLER

IBM Thomas J. Watson Research Center, Yorktown Heights, New York 10598

Received December 3, 1982; revised April 14, 1983

The phenomenon of Strong Metal–Support Interactions (SMSI) has been explained previously in terms of a chemical bonding between dispersed metal atoms and cations of certain supports. In this study, planar specimens of Pt/Al_2O_3, Rh/Al_2O_3, Pt/TiO_2, and Rh/TiO_2 were heated in hydrogen or oxygen and the resulting changes were observed by the technique of Nuclear Backscattering Spectrometry (together with electron microscopy). Significant and complex diffusion effects were found to occur, being dependent on the particular metal/support combination plus the environment and temperature to which it is exposed. This goes beyond the original mechanistic concept and the results suggest a much wider range of SMSI processes.

INTRODUCTION

The term Strong Metal–Support Interactions (SMSI) was coined by Tauster *et al.* (*1*) to describe an effect which they observed to occur when noble metals on TiO_2 were exposed to hydrogen or CO at 500°C. They found that the metals were incapable subsequently of adsorbing hydrogen or CO under standard conditions at 25°C and deduced that this was due to a chemical reaction between the dispersed metal and titanium cations on the surface of the support. They observed further (a) that the effect could be reversed by exposure to oxygen at 400°C; (b) that it could occur for a range of transition metal oxide supports, all of which were capable of reduction under these conditions (*2*); and (c) that it was not associated with loss of surface area of the support or gross sintering of the metal.

These initial observations have attracted widespread interest (*3*) because of their potential for elucidating how a support can function beyond its primary purpose of acting as a dispersant. A further fascination arises from the fact that titania-supported catalysts exhibit high activity for the CO + H_2 reaction (*4*) in spite of exhibiting SMSI effects when exposed to these gases individually.

It is the object of the present work to demonstrate that SMSI effects can be studied under well-defined conditions by the use of Nuclear Backscattering Spectrometry, in conjunction with planar specimens. The samples chosen for this purpose were Pt/TiO_2 and Rh/TiO_2 (because of their relevance to the original observations of Tauster *et al.*), together with Pt/Al_2O_3 and Rh/Al_2O_3.

Nuclear Backscattering Spectrometry (5, 6) (NBS)

This technique is often referred to as Rutherford Backscattering Spectrometry because, like the fundamental observations which led to the discovery of the atomic nucleus, it depends upon the interactions which occur when energetic charged particles undergo elastic Coulomb scattering by the nuclei of target atoms. The incident charged particles, which typically are He^+ in the few megaelectron-volts energy range, enter a target chamber as a collimated beam, typically 1 mm × 1 mm. The principle of the technique is that some of the He^+

---

[1] Permanent address: Catalyst Unit, Chemistry Division, AERE Harwell, Didcot, Oxfordshire OX11 0RA, England.

0021-9517/83 $3.00

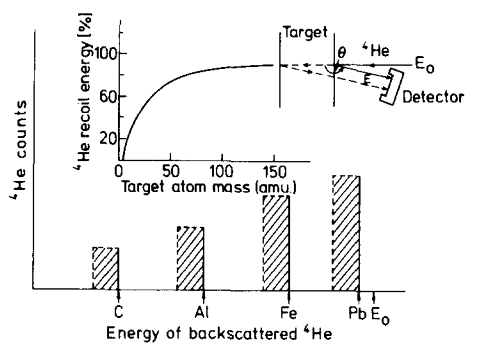

FIG. 1. Rutherford backscattering spectrometry. The experimental geometry is illustrated (top right-hand side) and the shaded areas represent typical backscattering yields for thin elemental films. For each profile, scattering of He^+ ions from the surface (solid lines) corresponds to the high-energy (right hand) side, while scattering from deeper in the film (dashed lines) populates the shaded region. The abscissa is essentially a scale of depth, while the counts per channel indicate the elemental concentration. The abscissa is also a scale of target atom mass, and the inset curve shows how the mass sensitivity of the technique diminishes for heavy target atoms.

ions will undergo close nuclear collisions with target atoms and consequently be scattered from the target with reduced energy. The energy retained by the He^+ ion after such collisions is dependent on the masses of the target atoms involved, being relatively high for heavy target atoms, such as Pt, and relatively low for light atoms such as Si, Al, and O. The energy spectrum of backscattered ions is measured by a surface barrier detector, mounted inside the target chamber, close to the bombarded specimen. A backward scattering angle (170°) is chosen in order to optimize discrimination between different target masses.

The main features of the technique are illustrated schematically in Fig. 1, which includes also an idealized indication of the spectrum which the surface barrier detector would yield from a target consisting of a few elements of widely differing masses. The most relevant features of the NBS technique with respect to its use in the present context may be summarized as follows:

(*i*) *It is mass sensitive.* When an ion of mass m_1, charge z_1, and energy E_0 is scattered at angle θ from a nucleus of mass m_2, charge z_2, its energy E as registered in the spectrum such as that of Fig. 1 will be given by

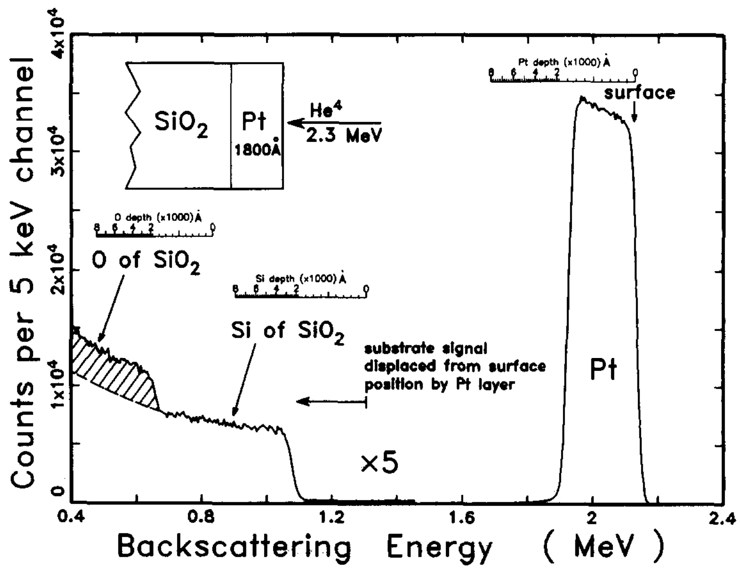

FIG. 2. Typical backscattering spectrum for 2300 keV He^+ ions incident on a sample consisting of Pt (~200 nm) deposited on a thick, flat SiO_2 substrate (support).

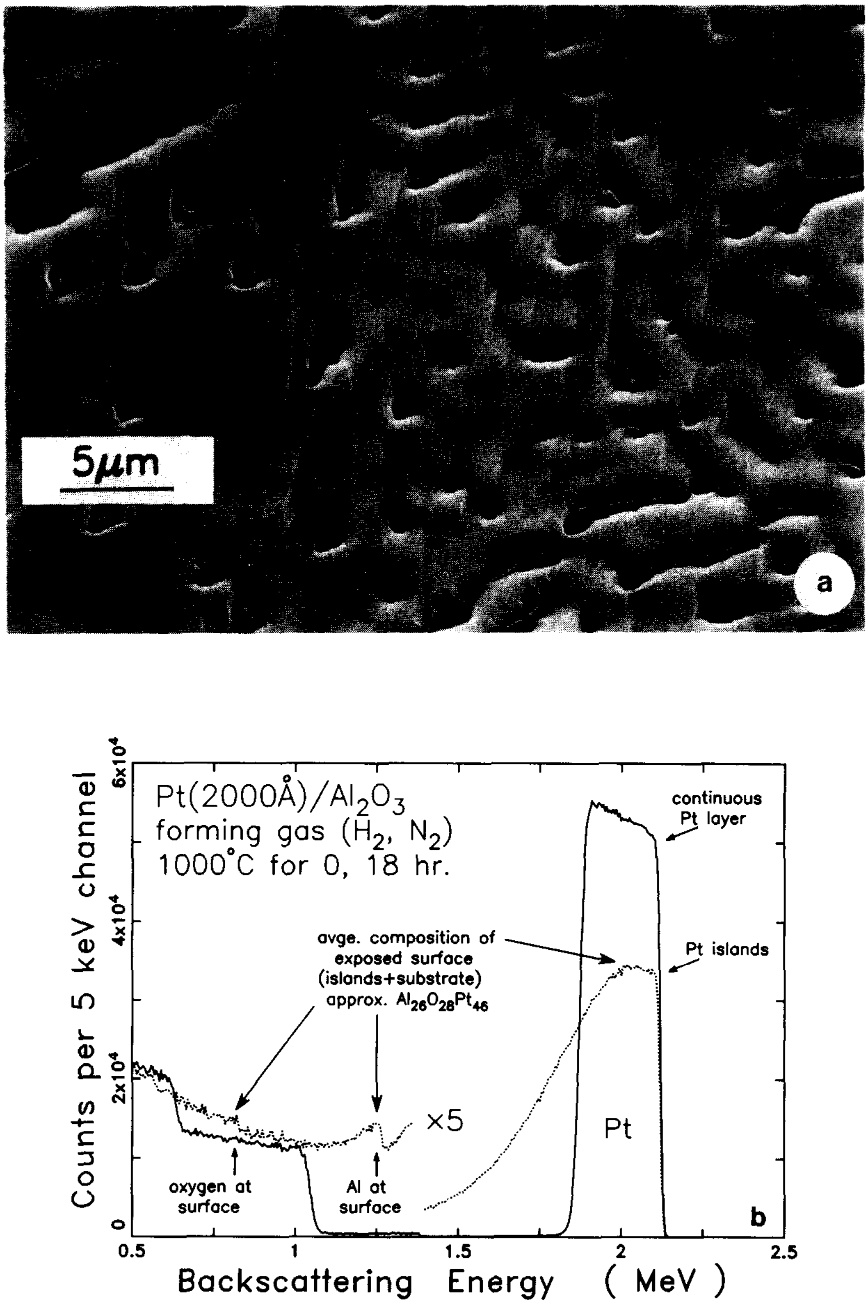

FIG. 3. (a) Scanning electron micrograph (SEM) for Pt/Al_2O_3 after exposure to 9/1 N_2/H_2 mixture "forming gas" (1000°C 18 h). The film has become discontinuous and significant substrate erosion has occurred. (b) NBS spectra from Pt/Al_2O_3 after exposure to forming gas at 1000°C for 0 h (solid line) and 18 h (dotted line). Irregular islands form, exposing areas of substrate. The average surface composition shows a depleted oxygen : aluminum ratio, consistent with reduction of the substrate and diffusion of the liberated Al into the Pt.

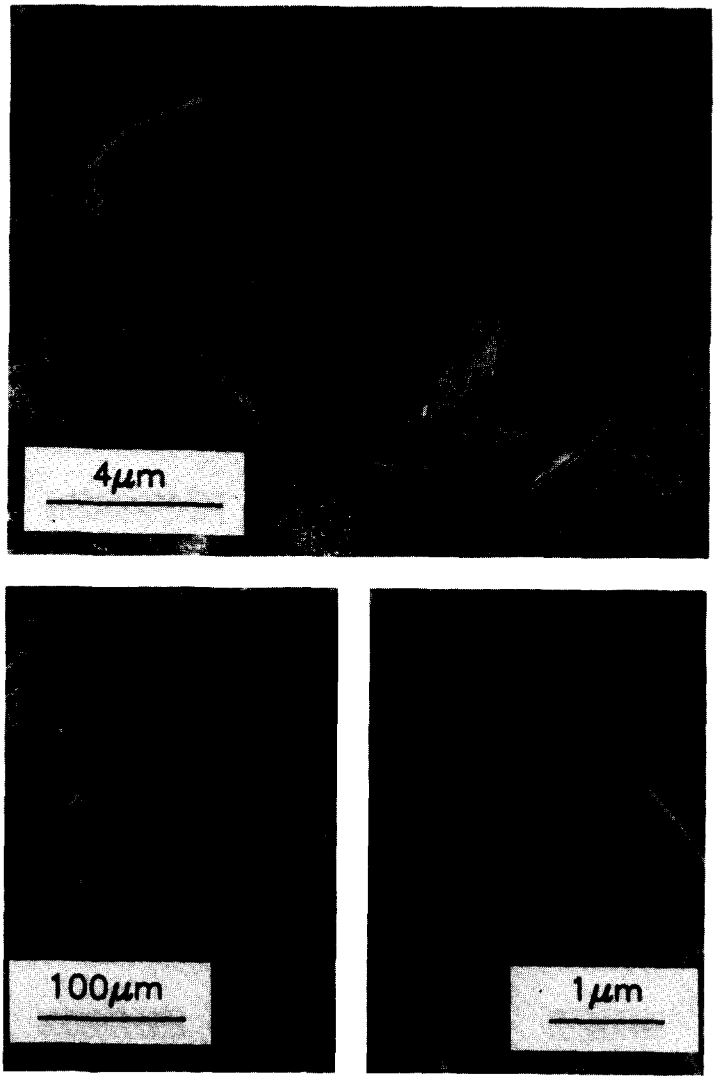
4μm
100μm
1μm

a

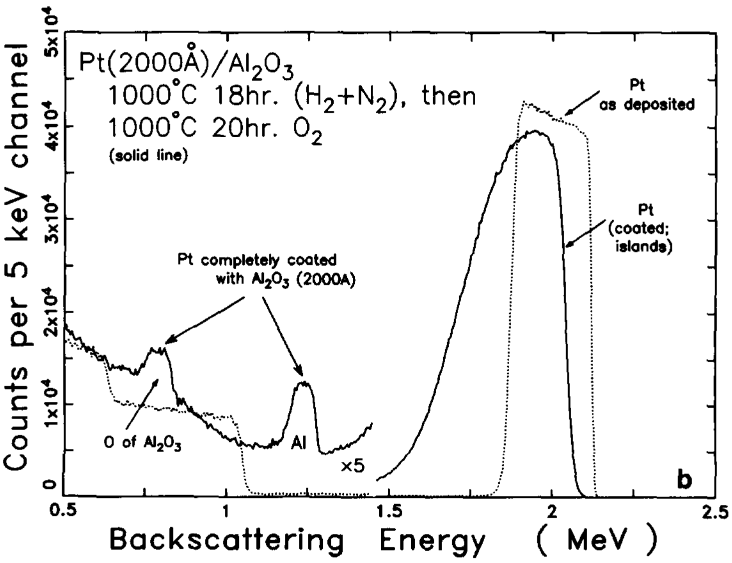
Pt(2000Å)/Al2O3
1000°C 18hr. (H2+N2), then
1000°C 20hr. O2
(solid line)
Pt as deposited
Pt (coated; islands)
Pt completely coated with Al2O3 (2000A)
O of Al2O3
Al
×5
b
Counts per 5 keV channel
0
1x10⁴
2x10⁴
3x10⁴
4x10⁴
5x10⁴
0.5
1
1.5
2
2.5
Backscattering Energy (MeV)

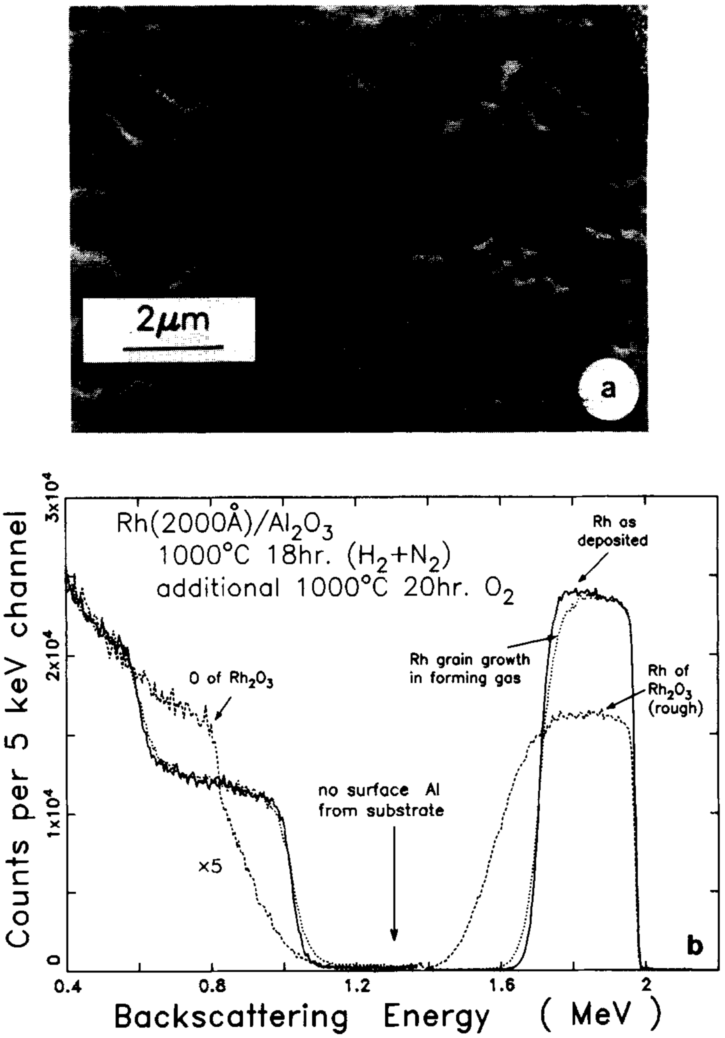

FIG. 5. (a) SEM for Rh/Al_2O_3 after exposure to forming gas (1000°C, 18 h) followed by oxidation (1000°C, 20 h). (b) NBS spectra for Rh/Al_2O_3 before (solid line) and after (dotted line) exposure to forming gas (1000°C, 18 h) and following subsequent oxidation (1000°C, 20 h O_2) (dashed line). No surface Al is found.

$$E = E_0\left(\frac{m_1\cos\theta + (m_2^2 - m_1^2\sin^2\theta)^{1/2}}{m_1 + m_2}\right)^2 \qquad (1)$$

The relationship of (E/E_0) with m_2 for He^+ scattering is shown in the inset to Fig. 1. It may be noted that the best mass resolution is obtained for low-mass elements, while for heavy elements, identification becomes more difficult.

(*ii*) *It is quantitative.* The number of helium ions scattered at energy E into a solid

FIG. 4 (a) SEM pictures for Pt/Al_2O_3 after exposure to forming gas (1000°C, 18 h) followed by oxygen (1000°C, 20 h). Each metal island appears to be bordered by a depression in the substrate. (b) NBS spectra from Pt/Al_2O_3 as deposited (dotted line) and after exposure to forming gas (1000°C, 18 h) and subsequent exposure to oxygen (1000°C, 20 h) (solid line). The O_2 treatment produces a layer of Al_2O_3 covering each Pt island.

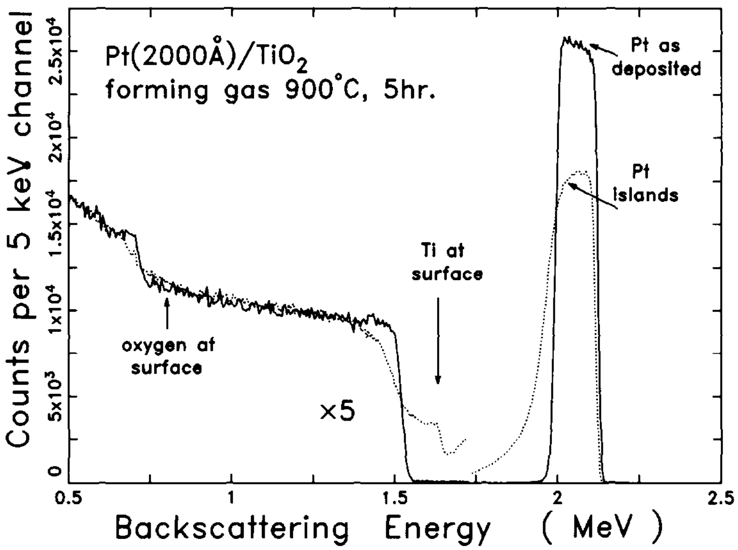

FIG. 6. NBS spectra for Pt/TiO$_2$ before (solid line) and after (dotted line) exposure to forming gas (900°C, 5 h). The spectra are consistent with the formation of metal islands, partly exposing the substrate. The average surface composition shows a depleted oxygen: titanium ratio.

angle $d\Omega$ subtended by the detector is directly proportional to the concentration of scattering nuclei of the corresponding species. For an elemental thin film, the area (total counts) C of a peak in the backscattering spectrum gives a direct measure of the quantity of material present N (atoms per cm^2). If the film thickness is only a few hundred nanometers or less, one may use the relationship

$$C = N\frac{d\sigma}{d\Omega} \cdot d\Omega \cdot q \qquad (2)$$

where q is the number of incident He$^+$ ions for the run, and $\frac{d\sigma}{d\Omega}$ is the differential cross section for Coulomb scattering given by

$$\frac{d\sigma}{d\Omega} = \left(\frac{Z_1 Z_2 e^2}{2E_0 \sin^2\theta}\right)^2 \cdot \frac{\left\{\left[1 - \left(\frac{m_1}{m_2} \times \sin\theta\right)^2\right]^{1/2} + \cos\theta\right\}^2}{\left[1 - \left(\frac{m_1}{m_2} \times \sin\theta\right)^2\right]^{1/2}} \qquad (3)$$

(*iii*) *It is rapid and nondestructive.* A typical spectrum can be accumulated in a few minutes. The helium ion dose (typically 10 μC in a 1-mm^2 spot) is not sufficient to heat the test area by more than a few degrees, or to cause radiation damage (in fact, NBS is routinely used in channeling geometry to evaluate the perfection of single crystal materials without causing sample deterioration).

(*iv*) *It provides elemental concentration vs depth profiles for thin films.* For example, if the outer film diffuses into the substrate (support) it gives rise to a broader spectrum, since the incoming He$^+$ ions will now lose a larger fraction of their initial energy before interacting with the most deeply diffused atoms, and will lose a further significant amount in reemerging from the deeper regions of the target. The energy loss of He$^+$ in all elements is well characterized and available in tabulated form (*7*). In practice normal incidence NBS has a typical resolution of 10 nm over several micrometers in depth. For smooth planar surfaces, however, grazing incidence can be used to give depth resolution of 1 or 2 nm, and in single crystal materials, channeling geometry can allow selective analysis of the surface monolayer.

(*v*) *It is sensitive to structural changes in the surface film.* For example, if a continuous film breaks up into globules, there will

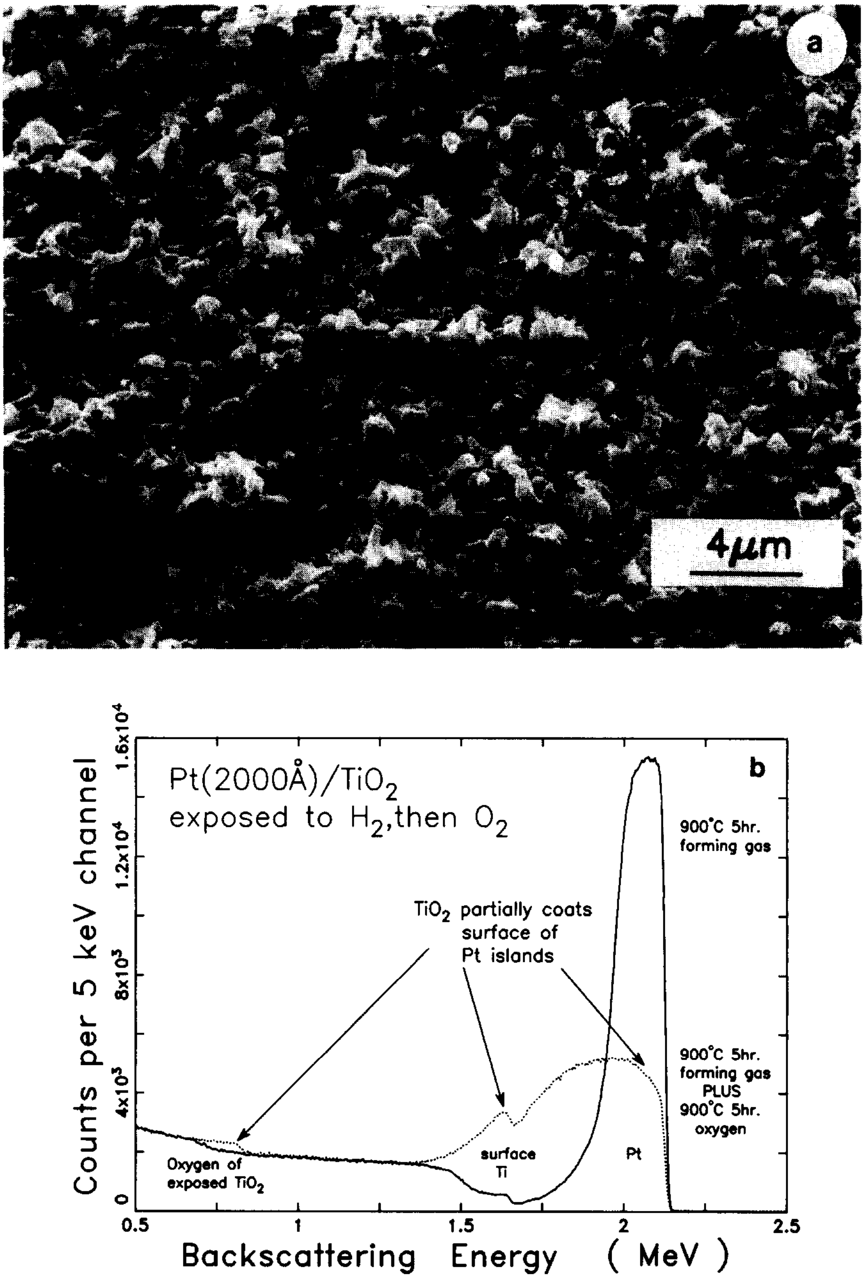

FIG. 7. (a) SEM for Pt/TiO_2 after exposure to forming gas (900°C, 5 h) followed by oxygen (900°C, 5 h). The film has become discontinuous. (b) NBS spectra for Pt/TiO_2 after exposure to forming gas (900°C, 5 h) (solid line) and following subsequent oxygen treatment (900°C, 5 h) (dotted line).

be a broadening on the low energy side of its NBS profile, together with a reduction in the overall profile height.

(*vi*) *It is sensitive to compositional changes in the film.* NBS is incapable of yielding direct chemical information, since it is sensitive only to the nuclear masses of the target atoms. However, it will be appreciated that if an elemental film under investigation becomes converted to a new com-

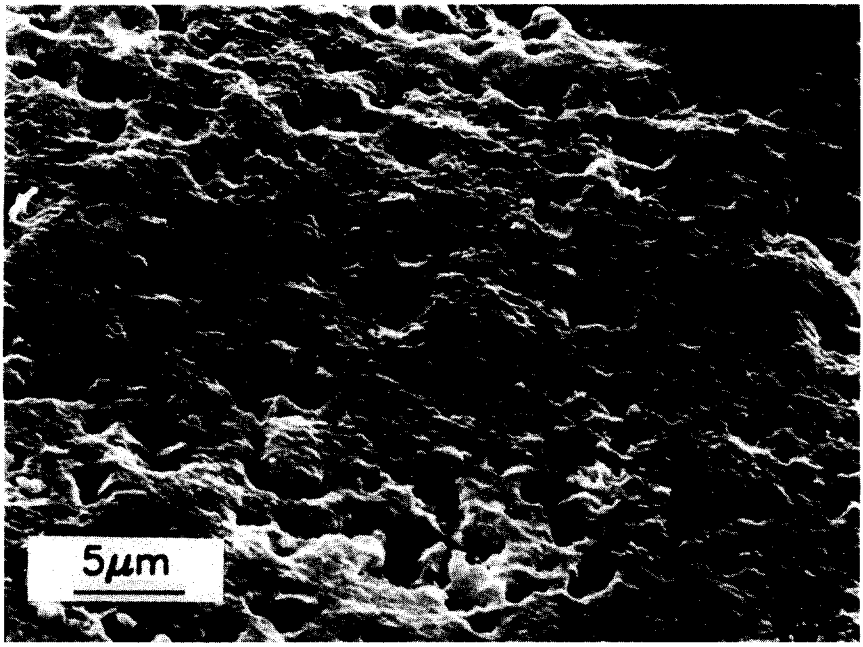

FIG. 8. SEM for Rh/TiO_2 after forming gas treatment (900°C, 5 h). The film has been appreciably disrupted.

pound by incorporation of additional atomic species, its backscattered spectrum will change in two respects: (a) it will become broader, and (b) there may be a new component in the spectrum from the additional atoms themselves. (One example of such a process would be the growth of an oxide layer on a metal surface.)

Hence NBS emerges as a technique which is suited to the quantitative, nondestructive examination of materials consisting of one or a few relatively heavy elements on substrates composed of low atomic number elements. These attributes account for its current widespread use in fundamental semiconductor technology research. Similarly, since many heterogeneous catalysts consist of a finite number of relatively heavy elements on light matrices, they too, when prepared ideally in the form of planar targets, should benefit from access to the technique. For example, Fig. 2 shows the NBS spectrum obtained from a Pt (200 nm)/SiO_2 specimen. Note the excellent separation between the ions backscattered from the Pt and from the elements of the SiO_2 substrate.

EXPERIMENTAL

Specimens were prepared by electron beam evaporation of thin films (200 nm) of the Pt and Rh on to single crystal Al_2O_3 (sapphire) and TiO_2 (rutile) substrates. These were heated in various gaseous environments, the TiO_2-supported ones at 900°C for 5 h and the Al_2O_3 ones at 1000°C for 18 h. Subsequently they were examined by NBS and scanning electron microscopy. X-Ray photoelectron spectroscopy, electron probe microanalysis, and scanning Auger microscopy were used occasionally to verify the most striking features described below.

RESULTS

The Consequence of Exposure to Hydrogen (or "Forming Gas" N_2/H_2: 9/1), Followed by Oxygen

Pt/Al_2O_3. This specimen was exposed to forming gas at 1000°C for 18 h, by which

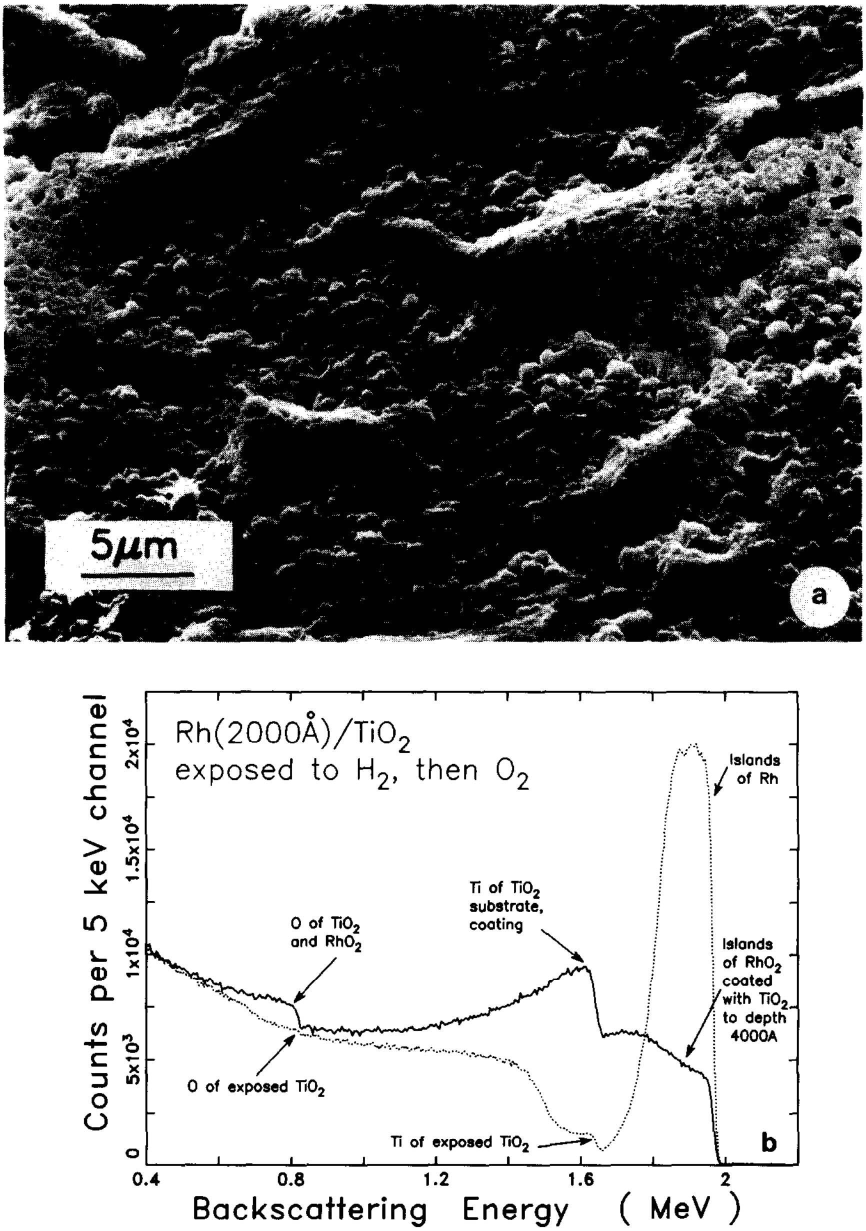

FIG. 9. (a) SEM for Rh/TiO_2 after forming gas treatment followed by oxygen exposure (900°C, 5 h). Disruption of the film is extensive. (b) NBS spectra for Rh/TiO_2 after forming gas treatment (dotted line) and following subsequent oxidation (900°C, 5 h) (solid line). Islands of Rh formed in the reduction stage become heavily coated with TiO_2 during oxidation of the Rh.

time there had been a break-up of the Pt film into islands (Fig. 3a). The NBS spectrum (Fig. 3b) confirmed that a significant proportion of the Al_2O_3 support had been uncovered, and that the islands contained both Pt and Al. The average surface layer composition indicates a net loss of oxygen in this process. After subsequent exposure of the sample to oxygen (also at 1000°C for 18 h) the islands (Fig. 4a) were now found (from the NBS spectrum, Fig. 4b) to be covered with an alumina film.

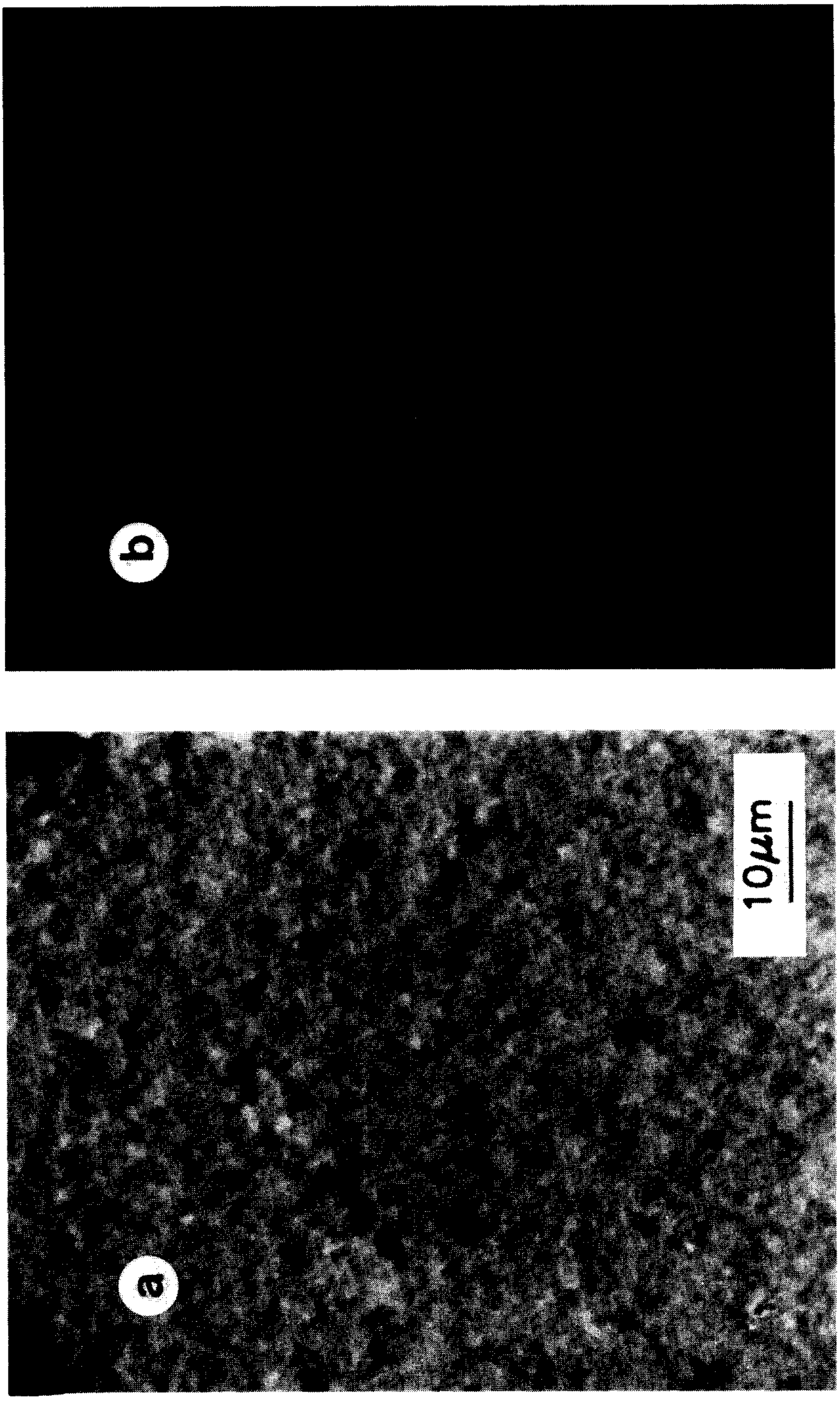

FIG. 10. Scanning electron micrographs for specimens after heat treatment in oxygen: (a) Pt/Al_2O_3, 1000°C, 18 h. (b) Rh/Al_2O_3, 1000°C, 18 h. (c) Pt/TiO_2, 900°C, 5 h. (d) Rh/TiO_2, 900°C, 5 h. No serious physical disruption of the films is observed. (Polishing marks are seen for the TiO_2 substrates.)

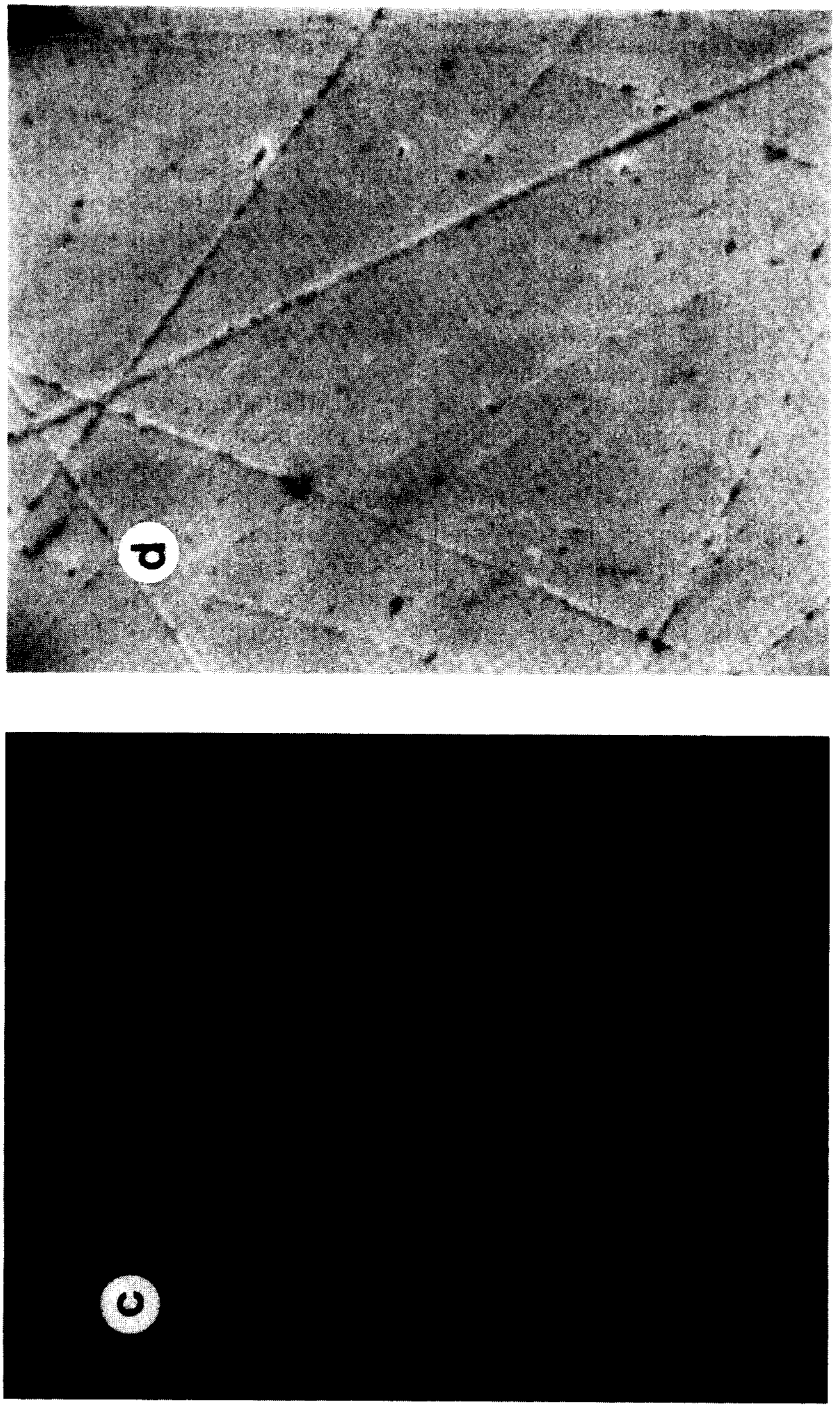

FIG. 10—*Continued.*

Rh/Al_2O_3. Under the same conditions as above, the Rh film became granular, but largely resisted physical disruption. On subsequent oxygen exposure the Rh oxidized, as confirmed from its NBS spectrum (Fig. 5b), but there was no evidence of Al on its surface, or of serious disruption of the film (Fig. 5a).

Pt/TiO_2. On reduction the Pt was found to show signs of breaking up. This is consistent with its NBS spectrum shown in Fig. 6. As in the case of the Pt/Al_2O_3, a net loss of oxygen in the average surface layers was evident. On subsequent oxygen exposure the disruption of the film became more pronounced (Fig. 7a). In addition, the Pt was found to be partially coated with titanium oxide from the support. This is consistent with the NBS spectrum shown in Fig. 7b.

Rh/TiO_2. On reduction the Rh was found to have become disrupted, as shown in Fig. 8. On subsequent oxidation this disruption was found to have become more severe (Fig. 9a) and to be associated with a significant titanium oxide coating, confirmed by the NBS spectrum shown in Fig. 9b.

The Consequences of Exposure to Oxygen

All four specimen types survived oxygen exposure without any serious physical disruption, as may be confirmed from the SEM pictures of Fig. 10. Chemically the Pt specimens remained unchanged, whereas the Rh specimens became oxidized, as may be confirmed from the NBS spectrum shown in Fig. 11.

DISCUSSION

Reduction and Subsequent Oxidation

We begin by attempting to relate these observations to the SMSI effects reported by Tauster *et al.* (*1, 2*) bearing in mind the more severe conditions to which we were obliged to subject our continuous-film planar specimens. For this reason we consider first the consequences of exposing the specimens to reducing conditions. We have shown that this can result in a break-up of the metal film into islands which in turn may incorporate elements from the support. (This would be expected to have a significant influence on the ability of a dispersed metal/support system to chemisorb hydrogen subsequently.)

Tentatively we propose the following mechanism to account for the observed effects. Chemisorption of H_2 on to noble metals is a well established method of producing atomic hydrogen, which may then diffuse through the noble metal layer to reduce the underlying support. The resultant modified support interface thereby will be rendered less compatible with the metal layer, which therefore will tend to lose contact and break up. This in turn facilitates access of hydrogen to the interface, local reduction of the support and subsequent interdiffusion between elements from the reduced support and the metal. We have shown above that Pt/Al_2O_3 breaks up more dramatically than Rh/Al_2O_3, an effect due presumably to the greater efficiency of Pt for the production of atomic hydrogen.

Hence we tend to go beyond the explanation for SMSI offered by Tauster *et al.* (*1*) by proposing an interdiffusional effect between the metallic phase and the support, which will alter the chemical composition of the metal and hence its subsequent hydrogen chemisorption behavior. It is relevant to note that Den Otter and Dautzenberg (*8*) reported the progressive inability of Pt on Al_2O_3 to chemisorb H_2 under standard conditions after exposure to H_2 at temperatures up to 700°C. They concluded that this was due to a Pt-assisted reduction of the Al_2O_3 support, leading to the formation of a Pt/Al alloy. Tatarchuk and Dumesic (*9*) studied the Fe/TiO_2 system, using iron overlayers (~5 nm thick) on TiO_2 films, characterized by transmission electron microscopy, conversion electron Mössbauer spectroscopy and X-ray photoelectron spectroscopy. They found that reduction at temperatures above ~600°C led to diffusion of iron into the titania support.

Tauster *et al.* (*1*) had made the further

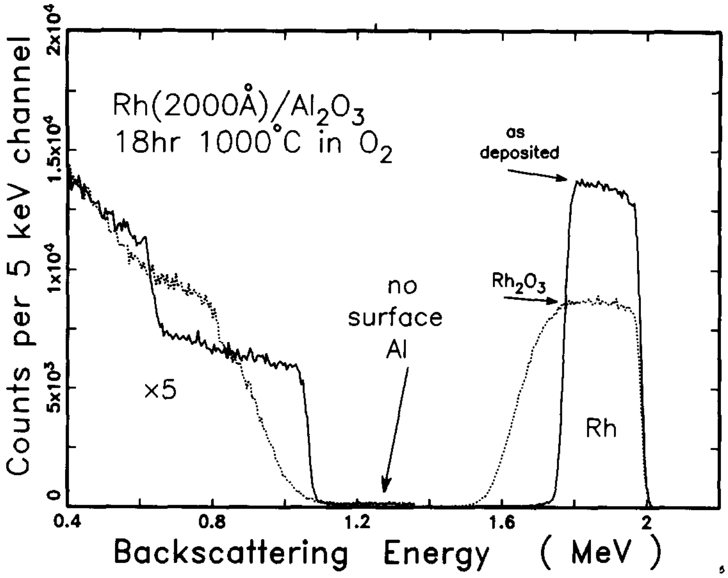

FIG. 11. Backscattering spectra from Rh/Al_2O_3 before (solid line) and after (dotted line) oxygen exposure at 1000°C. Simple conversion to Rh_2O_3 is evident.

interesting observation that high temperature H_2-deactivated TiO_2-supported catalysts could be regenerated by exposure to oxygen at ~400°C. This could be consistent with our mechanism, as indicated schematically for the Pt/Al_2O_3 system in Fig. 12. This illustrates how exposure to hydrogen at high temperature causes the Pt to break up into islets which incorporate elements diffused in from the support. Subsequent exposure to oxygen causes the Al to become reoxidized at the surface of the Pt, to produce Al_2O_3 islets and to leave active Pt exposed again, as indicated in Fig. 12a.

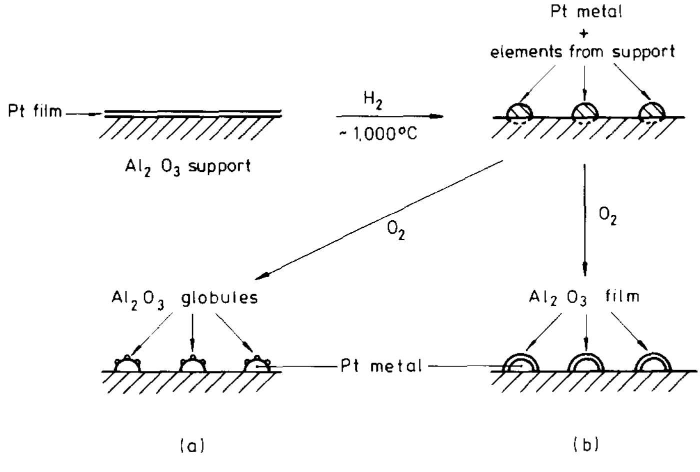

FIG. 12. The Pt/Al_2O_3 system. Proposed mechanism for degradation in a hydrogen atmosphere, and subsequent reactivation (a), or coating (b), after oxygen treatment. The critical distinction between paths (a) and (b) will depend on the amount of Al allowed to penetrate the Pt globules during the H_2 exposure.

However, if the initial reduction step is allowed to proceed for long periods then subsequent exposure to oxygen leads to a more or less continuous coverage of the Pt by Al_2O_3, as indicated in Fig. 12b and exemplified in the NBS spectrum shown in Fig. 4b.

This mechanism should be applicable also to Rh, but in this case we must face the added complication that the Rh will itself be oxidized during exposure to oxygen, as shown in Fig. 11. For this reason the NBS spectrum of Fig. 9b is consistent with a surface layer composed of a mixture of rhodium oxide and titania.

An analogous behavior to that described above has been reported by Cairns *et al.* (*10*) for a system composed of sequential continuous layers of Au/Fe/Au. It was found that exposure to an oxygen-containing environment at 350°C caused the gold layers to break up into islands and become covered with a layer of iron oxide.

CONCLUSIONS

It has been shown that the application of NBS and related techniques to model planar specimens can provide a significant insight into metal–support effects. In particular, it has been deduced that the electron transfer mechanism previously invoked to explain strong metal–support interactions should be extended in certain circumstances to include interdiffusion between the metal and its support.

REFERENCES

1. Tauster, S. J., Fung, S. C., and Garten, R. L., *J. Am. Chem. Soc.* **100,** 170 (1978).

2. Tauster, S. J., Fung, S. C., Baker, R. T. K., and Horsley, J. A., *Science* **211,** 1121 (1981).

3. See: "Metal-Support and Metal-Additive Effects in Catalysis" (B. Imelik, C. Naccache, G. Coudurier, H. Praliaud, P. Mériaudeau, P. Gallezot, G. A. Martin, and J. C. Védrine, Eds.), Elsevier Scientific, New York, 1982.

4. Vannice, M. A., and Garten, R. L., *J. Catal.* **56,** 236 (1979).

5. Ziegler, J. F., *in* "New Uses of Ion Accelerators," (J. F. Ziegler, Ed.). Plenum, New York, 1975.

6. Chu, W. K., Mayer, J. W., and Nicolet, M.-A., "Backscattering Spectrometry." Academic Press, New York, 1978.

7. Ziegler, J. F., "Helium, Stopping Powers and Ranges in All Elements." Pergamon, New York, 1977.

8. Den Otter, G. J., and Dautzenberg, F. M., *J. Catal.* **53,** 116 (1978).

9. Tatarchuk, B. J., and Dumesic, J. A., *J. Catal.* **70,** 308–322, 323–334, 335–346 (1981).

10. Cairns, J. A., Keep, C. W., Waite, R. J., Ziegler, J. F., and Tu, K. N., *Appl. Phys. Lett.* **24,** 36 (1974).